

Human short-wavelength-sensitive cone light adaptation

Andrew Stockman

Institute of Ophthalmology, University College London,
London, UK



Micha Langendörfer

Forschungsstelle für Experimentelle Ophthalmologie,
Tübingen, F.R.G.



Lindsay T. Sharpe

Institute of Ophthalmology, University College London,
London, UK



The cone-driven visual system is able to regulate its sensitivity effectively from twilight to bright sunlight. On the basis of a novel combination of short-wavelength-sensitive (S-) cone measurements of temporal sensitivity *and* temporal delay, we show that S-cone light adaptation is achieved not only by trading unwanted sensitivity for speed but also by an additional process that counterintuitively *increases* the overall sensitivity as the light level rises. Our results are consistent with comparable middle-wavelength-sensitive (M-) cone measurements made in protanopic observers and can be accounted for by the same two-parameter model developed to account for the M-cone data (A. Stockman, M. Langendörfer, H. E. Smithson, & L. T. Sharpe, 2006). Each stage of the model can be linked to molecular mechanisms occurring within the photoreceptor: the speeding up to increases in the rates of decay of active and messenger molecules, the unexpected sensitivity increases to increased rates of molecular resynthesis and changes in channel sensitivity, and the sensitivity decreases to bleaching. Together, these mechanisms act to maintain vision in an optimal operating range and to protect it from overload.

Keywords: light adaptation, S-cones, temporal sensitivity, phase lags, protanopes, sensitivity regulation, visual transduction

Citation: Stockman, A., Langendörfer, M., & Sharpe, L. T. (2007). Human short-wavelength-sensitive cone light adaptation. *Journal of Vision*, 7(3):4, 1–17, <http://journalofvision.org/7/3/4/>, doi:10.1167/7.3.4.

Introduction

The human cone visual system is able to operate over a range of $>10^8$ environmental light levels despite the much more limited response range of constituent neurons in the visual pathway. The process by which it achieves this is known as light adaptation. Below bleaching levels, the principal mechanism of cone light adaptation is the speeding up of the visual response and the concomitant shortening of the visual integration time with increasing light level so that observers become relatively more sensitive to flicker of higher temporal frequencies under brighter conditions. These sensitivity changes are readily apparent in temporal modulation threshold data, which are frequently used to model human cone light adaptation (e.g., De Lange, 1958, 1961; Green, 1968; Kelly, 1961, 1974; Matin, 1968; Sperling & Sondhi, 1968; Tranchina, Gordon, & Shapley, 1984; Watson, 1986). Modulation sensitivity data, however, provide only a partial picture of the effects of light adaptation. A more complete picture requires knowledge of the accompanying reductions in visual delay (e.g., Cavonius & Estévez, 1980; Lit, 1949; Pulfrich, 1922; Rock & Fox, 1949; Wilson & Anstis, 1969).

In this work, we combine modulation sensitivity with phase delay measurements for conditions under which

detection is mediated by the short-wavelength-sensitive (S-) cones. This work complements and extends our previous work, in which we measured the adaptation-dependent changes in sensitivity and phase delay for detection mediated by the middle-wavelength-sensitive (M-) cones (Stockman, Langendörfer, Smithson, & Sharpe, 2006). For the M-cone measurements, we found that the adaptational changes could be explained by a simple model that requires just two adaptation-dependent parameters to account qualitatively for the effects of light adaptation over 5 log units of intensity: one that controls the speed of the response and the other that controls the overall sensitivity. Surprisingly, however, increases in light level below bleaching levels cause *increases* in overall sensitivity, which oppose the sensitivity losses due to the shortening integration time. From a psychophysical or systems perspective, such increases seem counterintuitive because the primary requirement of light adaptation is to decrease the sensitivity of the visual system to increasingly intense lights. The need for sensitivity increases becomes clear, however, when the perspective is changed to the molecular level: They reflect essential processes that restore depleted messenger molecules and increase the availability of limited ion channels. Without these processes, the visual response would quickly saturate as the molecules or channels run out (see the [Discussion](#) section). Here, we extend our measurements

and test our model under conditions that isolate the S-cone response.

For the previous M-cone measurements, we used protanopes, who lack long-wavelength-sensitive (L-) cones, so that we could measure the isolated M-cone response over an extended range of intensity levels (alternatively, we could have used deuteranopes and measured the L-cone response). In addition, we measured phase delays binocularly so that we could independently manipulate the level of M-cone adaptation in both eyes. S-cone measurements are inherently more straightforward. Thanks to the substantial spectral sensitivity differences between the S-cones and the other cones, the isolated S-cone response can be monitored over an extended range of S-cone adaptation levels in normal trichromatic observers simply by presenting the S-cone target on a very intense long-wavelength adapting background. Such a background not only suppresses the M- and L-cones so that the S-cone response can be isolated but also keeps the adaptive states of the M- and L-cones constant as that of the S-cones is varied. Consequently, the delay of the S-cones can be measured relative to that of the L- or M-cones in the same eye. The downside of monitoring the S-cone response on an intense long-wavelength field is that it saturates at moderate adaptation levels, which restricts the measurements to an approximately 3.3 log unit range.

Compared with the other cones, S-cone temporal modulation sensitivity is relatively impoverished at higher temporal frequencies (e.g., Green, 1969; Kelly, 1974; Stockman, MacLeod, & DePriest, 1991; Wisowaty & Boynton, 1980) but less so when the S-cone signal is detected via the luminance or achromatic pathway (Stockman et al., 1991; Stockman, MacLeod, & Lebrun, 1993). The existence of this S-cone input to luminance has been contentious, but it now seems clear that the S-cones do make a small luminance contribution when the S-cone response is enhanced (relative to the responses of the L- and M-cones) by intense long-wavelength adaptation (Lee & Stromeyer, 1989; Stockman, MacLeod, & DePriest, 1987, 1991). Indeed, the phase measurements reported here depend crucially on the S-cone signal behaving like a luminance signal because our technique requires the S-cone signal to flicker photometrically cancel M- or L-cone signals (i.e., for the different cone signals to interfere destructively). S-cone phase delays measured in this way before have revealed that the S-cone signal is inverted in sign with respect to the M- and L-cone signals so that it must be in-phase with them to cancel them at very low frequencies (Lee & Stromeyer, 1989; Stockman et al., 1987, 1991).

Our combined modulation sensitivity and phase delay data for S-cone-detected stimuli allow us to model the light adaptation of an isolated cone system over a substantial intensity range in normal trichromatic

observers. Moreover, they confirm our previous M-cone data and model, based on measurements in protanopic observers.

Methods

Subjects

Three male subjects, A.S., M.L., and L.T.S., served as observers in these experiments. M.L. is protanopic when tested with a standard (2.5° visual diameter viewing field) Nagel Type I anomaloscope (i.e., he could match spectral lights in the red–green range by adjusting only the relative intensities of the lights). Molecular genetic analyses reveal that he has two genes in the opsin gene array on his X chromosome that produce photopigments with essentially identical spectral sensitivities (Sharpe et al., 1998). A.S. and L.T.S. are phenotypically and genotypically color normal. Both have a normal M-cone gene with the alanine polymorphic variant at position 180 and a normal L-cone gene with the serine variant at position 180 (Sharpe, Stockman, Jagla, & Jägle, 2005).

Apparatus

A conventional Maxwellian-view optical system with a 2-mm entrance pupil illuminated by a 75-W Xe and a 100-W Hg arc lamp was used for these experiments. Wavelengths were selected using interference filters with full-width at half-maximum (FWHM) bandwidths of between 7 and 11 nm (Ealing or Oriol) or Jobin-Yvon H-10 monochromators with 0.5-mm slits, the spectral outputs of which were a triangular function of wavelength with FWHM bandwidths of 4 nm. The radiance of each beam could be controlled by the insertion of fixed neutral density filters (Oriol) or by the rotation of circular, variable neutral density filters (Rolyn Optics). Sinusoidal modulation was produced by the pulse-width modulation of fast, liquid crystal light shutters (Displaytech) at a carrier frequency of 400 Hz (which is much too fast to be resolved so that subjects saw only the sinusoidal intensity variation produced by the pulse-width modulation). Each shutter had rise and fall times of less than 50 μ s and could produce sinusoidal modulations from 0% to 92%.

Calibration

The radiant fluxes of the test and adapting fields were measured daily at the plane of the observer's entrance pupil with a radiometer (Graseby Electronics), which had been cross-calibrated with comparable devices traceable to U.S. and German national standards. Interference filters were spectrally calibrated in situ with a spectroradiometer (Gamma Scientific).

Experimental conditions

Modulation sensitivity measurements

Modulation sensitivities were measured monocularly. A 4°-diameter, 440-nm target was superimposed in the center of a larger, 9°-diameter background of 620 nm and 12.00 log quanta s⁻¹ deg⁻² (M.L. and A.S.) or of 610 nm and 12.00 log quanta s⁻¹ deg⁻² (L.T.S.). These combinations of target and background wavelengths were chosen to ensure that the 440-nm flicker was detected by the S-cones (as has been demonstrated in several previous publications; Stockman et al., 1991, 1993; Stockman & Plummer, 1998). The target was varied from 6.80 to 10.30 log quanta s⁻¹ deg⁻², as noted in the keys of the figures shown below. These values are time averaged. The values in the keys in brackets give the combined effect on the S-cones (in terms of equivalent 440-nm quanta) of the violet target *plus* the orange background if it differs significantly from the effect of the target alone. Measurements could not be made above 10.30 log quanta s⁻¹ deg⁻² because above that level, the S-cone response saturates (e.g., Mollon & Polden, 1977; Stromeyer, Kronauer, & Madsen, 1979).

The central feature of these experiments is that the orange background is intense enough to hold the adaptive states of the M- and L-cones approximately constant as the radiance of the 440-nm target is varied, which itself has little or no direct effect on the M- or L-cones. Changes in S-cone sensitivity and phase should, thus, primarily reflect the effects of changes in S-cone excitation.

Monocular phase lag measurements

For these experiments, the S-cone target and the background field were identical to those used to measure modulation sensitivities: A 4°-diameter, 440-nm target was superimposed in the center of a larger, 9°-diameter, 610- or 620-nm background. In addition, a second 4°-diameter target of 600 nm and 11.36 log quanta s⁻¹ deg⁻² (M.L.) or of 610 nm and 10.66 (A.S.) or 10.77 (L.T.S.) log quanta s⁻¹ deg⁻² was superimposed on the 440-nm target, which excited only the M- or the L-cones. The differences between these targets reflect sensitivity differences between the observers: M.L. lacks L-cones—so that a shorter wavelength and brighter target was needed for the reference flicker to be visible at 25–30 Hz—and A.S. was slightly more sensitive than L.T.S. For the phase measurements, one modulated target excited S-cones, whereas the other excited M-cones, L-cones, or both.

Binocular phase lag measurements

For these experiments, carried out only on observer L.T.S., the target and field stimuli were identical to those used to measure modulation sensitivities, but they were presented to *both* left and right eyes. In each eye, a 4°-diameter, 440-nm target was superimposed in the

center of a larger, 9°-diameter, 610-nm background. The levels of the 440-nm target in the right eye were varied in the same way as in the monocular measurements. The level of the 440-nm target in the left (reference) eye was fixed at 8.80 log quanta s⁻¹ deg⁻².

Experimental procedures

Subjects interacted with the computer-controlled Maxwellian-view optical system by means of an eight-button keypad and received instructions and information from the computer by means of tones and a voice synthesizer. The observers light-adapted to the target and adapting fields for at least 3 min prior to any data collection. Temporal frequencies were presented in 2.5-Hz steps.

Modulation threshold measurements

Modulation sensitivities were measured by the method of adjustment. Modulation, which is defined as $(I_{\max} - I_{\min}) / (I_{\max} + I_{\min})$ is given in terms of S-cone excitation. Relative cone excitations were calculated using the Stockman and Sharpe (2000) cone spectral sensitivities. An alternative way of defining threshold is in terms of the flicker amplitude, which is simply the difference between I_{\max} and I_{\min} . Amplitudes are given below in units of log quanta s⁻¹ deg⁻² at 440 nm.

The subject was presented with the flickering stimulus and was asked to adjust its modulation until the flicker appeared just at threshold to determine modulation sensitivity. Only the modulation of the 440-nm target was varied; the 610-nm background remained steady. On a single run, three threshold settings were made at each temporal frequency. The data are averaged from four separate runs.

Phase lag measurements

Phase lags were measured using an extension of flicker photometry, in which the subject was instructed to vary the relative phase as well as the modulation of the two targets to abolish or minimize the subjective flicker. By pressing keys, the subject could advance or retard the phase. If the null covered an extended range of phase delays, which was usually the case if one of the two signals was weak, subjects were instructed to set the middle of the range. Three phase settings were made at each temporal frequency in a single experimental run. At least four separate experimental runs were carried out for each condition.

The principle behind using phase adjustments to measure relative perceptual delays is illustrated in Figure 2 of Stockman et al. (2006). Flicker interactions between S-cone and M- or L-cone flicker can sometimes be detected even when the S-cone flicker is itself below modulation

threshold (Stockman et al., 1993). Thus, S-cone phase delays can sometimes be measured at frequencies at which the S-cone modulation cannot.

Results

S-cone modulation sensitivities

The bottom left panels of Figures 1, 2, and 3 show the S-cone modulation sensitivity curves for A.S., L.T.S., and M.L., respectively. For each subject, increasing the adaptation level from the lowest level up to approximately 9.30 log quanta s⁻¹ deg⁻² causes a relative increase in the sensitivity to higher frequencies and, thus, a broadening of the functions. Between approximately 9.30 and 9.80 log quanta s⁻¹ deg⁻², the improvements for A.S. and M.L. are modest, but some larger improvement occurs for L.T.S. Thereafter, the S-cone system saturates so that at the highest level of 10.30 log quanta s⁻¹ deg⁻², the functions are atypical. Because we were also unable to

measure phase delays at 10.30 log quanta s⁻¹ deg⁻², these threshold data were excluded from the modeling discussed below.

The S-cone modulation sensitivity data for M.L. are primarily bandpass except for the one measured at the lowest adaptation level at which he could detect modulation (7.21 log quanta s⁻¹ deg⁻²). In contrast, the functions for A.S. and L.T.S. are more low pass with a slight inflection at 7.5 Hz (see also right panels). Evidence that this inflection separates a distinct low-pass S-cone chromatic mechanism, which is more sensitive at low frequencies, and a bandpass S-cone luminance or achromatic mechanism, which is more sensitive at middle and high frequencies, was presented in Stockman et al. (1991).

If the modulation sensitivities remain constant as the light level is increased, then Weber's law ($\Delta I/I = k$) holds. In general, Weber's law behavior is found at lower frequencies at intermediate radiances and at all frequencies at the highest radiances below the saturating level. Between the two highest levels, modulation sensitivity falls at some frequencies, which is consistent with saturation. Saturation under comparable conditions has

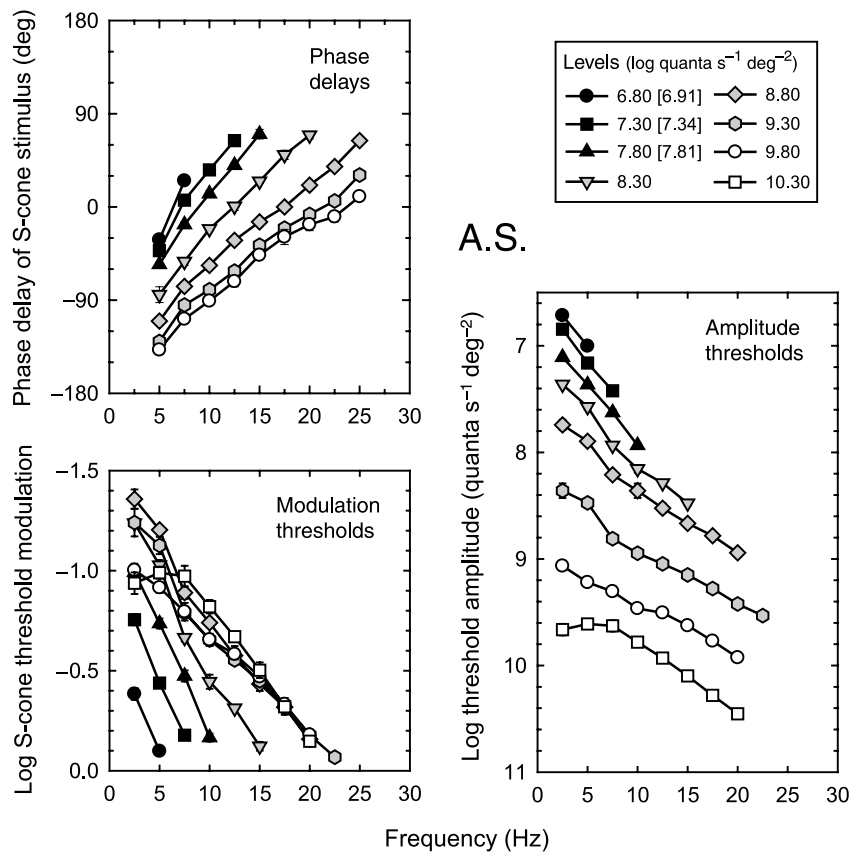


Figure 1. Mean data for A.S. Lower left panel: logarithmic S-cone modulation thresholds plotted against frequency. Right panel: thresholds replotted as logarithmic amplitude thresholds in quanta s⁻¹ deg⁻² at 440 nm. Note that the vertical scale is halved. Upper left panel: phase delays of S-cone signals plotted relative to those of L/M-cone signals. The S-cone adaptation level given in terms of log quanta s⁻¹ deg⁻² at 440 nm was varied according to the key. The values in brackets indicate the combined effect on the S-cones (in terms of equivalent 440-nm quanta) of the violet target plus the orange background, if it differs from the effect of the target alone.

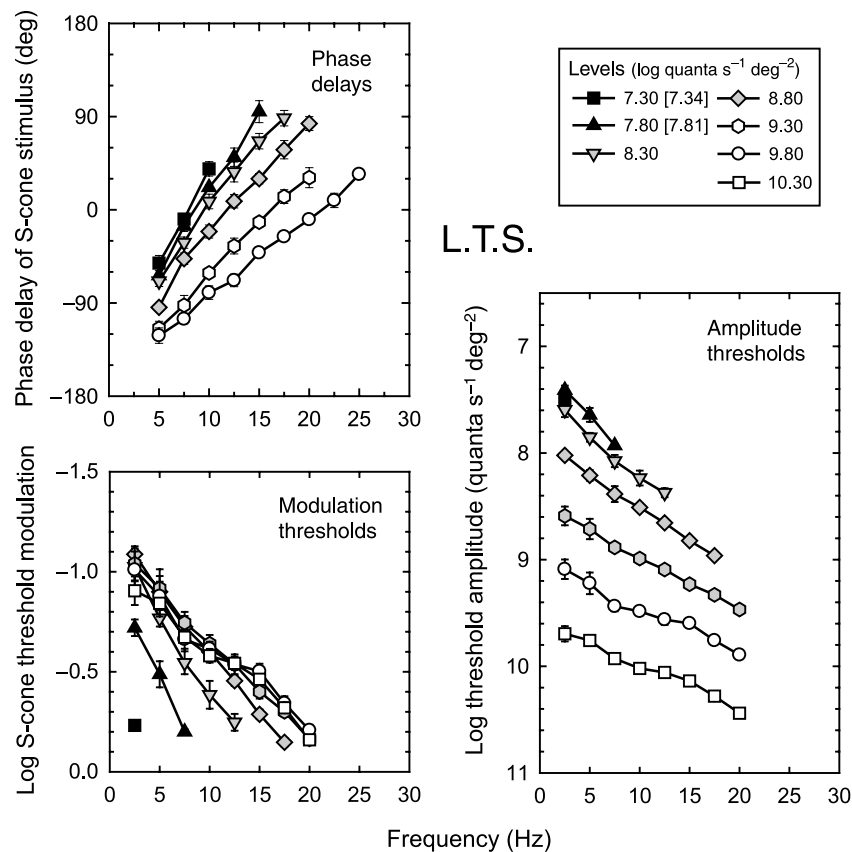


Figure 2. Mean threshold and phase delay data for L.T.S., the details of which are explained in the caption for Figure 1.

been reported before (Mollon & Polden, 1977; Stockman & Plummer, 1998; Stromeyer et al., 1979).

A helpful way of visualizing the modulation sensitivity data is to plot them as threshold amplitudes ($I_{\max} - I_{\min}$), as shown in the right-hand panels of Figures 1, 2, and 3 for A.S., L.T.S., and M.L., respectively. This type of plot helps highlight those levels between which the change in background has no effect on the threshold amplitude (i.e., when $\Delta I = k$). Such behavior is known as high-frequency linearity. In contrast to the M-cone data (Stockman et al., 2006), which could be measured at much higher adaptation levels, there is no direct evidence for high-frequency linearity in our S-cone measurements because none of the data merge at higher frequencies. This difference is due mainly to the temporal acuity for S-cone-detected flicker being much lower than that for L- or M-cone-detected flicker (e.g., Brindley, Du Croz, & Rushton, 1966).

Despite the substantial differences between the shapes of the sensitivity curves for the three subjects, the changes in sensitivity between adaptation levels can be accounted for by the same model (see Figure 4).

S-cone monocular phase lags

The upper left panels of Figures 1, 2, and 3 show the relative phase delays between S-cone and L/M-cone

flicker for A.S., L.T.S., and M.L., respectively. As noted above, the radiances of the long-wavelength background and target were held constant as the radiance of the 440-nm target was increased. Relative to the L/M-cone signals, the S-cone signals speed up substantially with adaptation. At 10 Hz, for example, the signal advances by nearly 180° between 6.79 and 9.70 log quanta (or, in time, by 50 ms).

Owing to the presence of the intense orange background, the M- or L-cones are always more light-adapted than the S-cones. Consequently, the S-cone signals are always slower than the M-cone signals so that the S-cone phase delays increase with frequency. In addition to differential cone adaptation, the phase delays might also arise because the S-cone signal is subject to more postreceptoral filtering (see below). An unusual feature of the S-cone phase delays is that they extrapolate toward -180° at 0 Hz rather than toward 0° , which indicates that the sign of the S-cone signal is inverted with respect to the sign of the M-cone signal (Lee & Stromeyer, 1989; Stockman et al., 1987, 1991).

Notice that there are several examples of S-cone phase delays that are measurable, even though the S-cone modulation is below threshold. A particular example is the lowest level of 6.79 log quanta $s^{-1} \text{ deg}^{-2}$ for M.L. Other examples for all three observers include phase delays that can be set above the S-cone CFF. Under optimal conditions, S-cone and L- or M-cone flicker

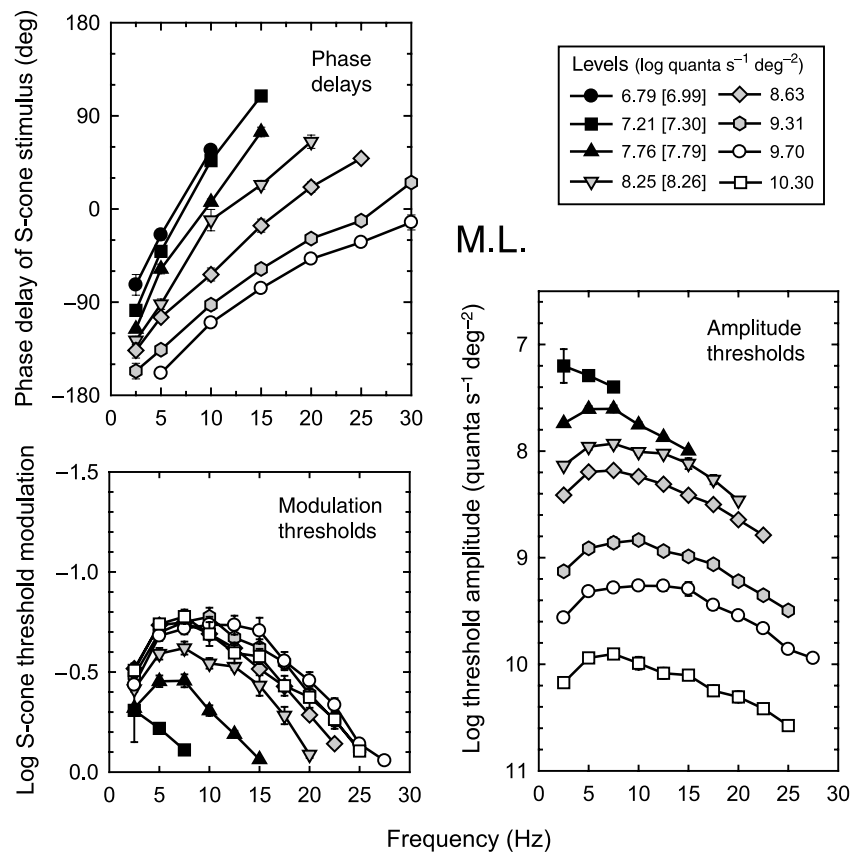


Figure 3. Mean threshold and phase delay data for M.L., the details of which are explained in the caption for Figure 1.

interactions can be seen at frequencies as high as 40 Hz (Stockman et al., 1993). The phase delays shown here are consistent with comparable data obtained by Stockman et al. (1991).

Light adaptation models

Having both phase delay and amplitude data allows us to better constrain and test models of human light adaptation because any candidate model must simultaneously account for both types of data. Our goal in this article, as in our previous article on M-cone adaptation (Stockman et al., 2006), is to find a simple, mainly *descriptive* model of adaptation that requires just one or two adaptation-dependent parameters.

The amplitude and phase delay data for all three subjects show frequency-dependent changes that are broadly consistent with a speeding up of the visual response and a shortening of the visual integration time. Accordingly, we first take the classic approach of modeling the changes by shortening the time constants (τ) of one or more (n) cascaded leaky integrating stages (or buffered RC circuits; see, e.g., Watson, 1986). This approach remains relevant in the context of cascaded molecular processes because a leaky integrator is comparable to a first-order biochemical reaction. The formula

for the amplitude response, $A(f)$, of n cascaded leaky integrators is

$$A(f) = \tau^n \left[(2\pi f \tau)^2 + 1 \right]^{-\frac{n}{2}}, \quad (1)$$

and for the phase response, $P(f)$, the formula is

$$P(f) = n \tan^{-1}(2\pi f \tau), \quad (2)$$

where f is the frequency in cycles per second (hertz) and τ is the time constant in seconds. When the frequency, f , is high relative to $1/(2\pi\tau)$ (the so-called cutoff or corner frequency of a filter in hertz), the amplitude and phase are independent of changes in the time constant. Thus, a cascade obeys what is termed “high-frequency linearity.” By contrast, when the frequency is low, the loss of sensitivity is proportional to the shortening of the time constant raised to the power of the number of integrators. Therefore, a cascade that obeys high-frequency linearity can, in principle, also obey Weber’s law, if the change in time constants is appropriately matched to the increase in luminance.

Our phase delay measurements are relative data; thus, we must apply our modeling to the *changes* in phase delay and the *changes* in threshold amplitude between the

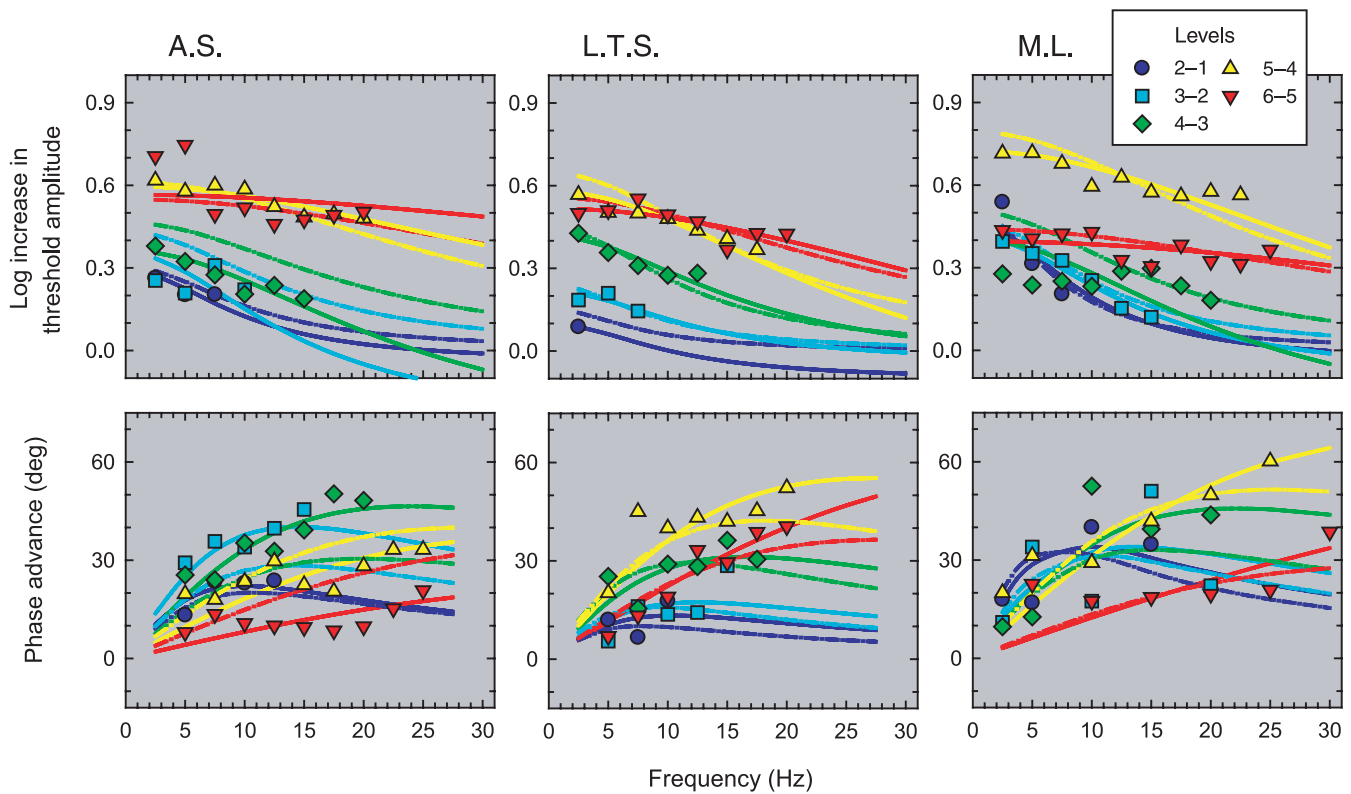


Figure 4. Simultaneous fits of either the one-adaptation-dependent-parameter model (dashed lines) or the two-adaptation-dependent-parameter model (continuous lines) to the amplitude differences (symbols, upper row) and phase delay differences (symbols, lower row) between successive levels for A.S. (left column), L.T.S. (middle column), and M.L. (right column). The levels are noted in the key; the same color code is used for the symbols and for the model predictions.

six successive levels from approximately 7.30 to 9.80 $\log \text{ quanta s}^{-1} \text{ deg}^{-2}$. Figure 4 shows the amplitude (upper row) and phase delay changes (lower row) for A.S. (left column), L.T.S. (middle column), and M.L. (right column).

In optimizing the model parameters, the time constants of each of the n filters were varied simultaneously, thus altering the threshold amplitudes according to Equation 1 and the phase delays according to Equation 2. Allowing the time constants of each filter to vary independently did not significantly improve the predictions. The phase and amplitude data were weighted so that their influence was approximately equal (otherwise, one set of data or the other set would dominate). When n was allowed to take on noninteger values, the best fitting models for the subjects were $n = 1.61$ (A.S.), $n = 2.98$ (L.T.S.), and $n = 3.67$ (M.L.). On the basis of these preliminary fits, we have chosen $n = 3$, which is also consistent with our M-cone article. We emphasize, however, that n is poorly constrained by the fit because increases in n can be offset by decreases in τ and vice versa. The time constants of fits for $n = 2, 3$, and 4 are compared in the Discussion section.

The model fits for three leaky integrators are shown by the dashed lines, which are color coded in the same way as the symbols. As can be seen, the model based on only filters does a fairly good job of accounting for the

changes in amplitude thresholds and phase delays with adaptation for L.T.S. and M.L., but there are clear discrepancies for A.S. Relative to the null model that there is no change in amplitude or phase between levels (i.e., that all the values in Figure 4 are zero), the model accounts for 96.05% of the threshold amplitude and 87.12% of the phase variance for A.S., 98.96% of the threshold amplitude and 95.51% of the phase variance for L.T.S., and 96.25% of the threshold amplitude and 91.01% of the phase variance for M.L. Relative to the mean of each set of data, the model accounts for 70.60% of the threshold amplitude and only 25.51% of the phase variance for A.S., 89.65% of the threshold amplitude and 77.16% of the phase variance for L.T.S., and 74.40% of the threshold amplitude and 50.65% of the phase variance for M.L. In general, the model predictions are good, except for the phase predictions for A.S. and M.L. However, given that this model has just a single adaptation-dependent parameter, the predictions are impressive.

We next tried to improve the model predictions, as we did when modeling our M-cone data (Stockman et al., 2006), by adding an extra adaptation-dependent parameter to the model. A biologically plausible addition, certainly in terms of the molecular mechanisms described above, is to allow a frequency-independent “turning up or down” of

the visual response by multiplicatively scaling the amplitude thresholds (i.e., by shifting the logarithmic functions threshold amplitude functions vertically without changing their shape) while leaving the phase delays unaffected. The two-adaptation-dependent-parameter model fits are shown by the continuous lines in Figure 4, which are again color coded in the same way as the symbols. The predictions are better for all three subjects, particularly for A.S. Relative to the null model that there is no change in amplitude or phase between levels, the two-parameter model accounts for 98.11% of the threshold amplitude and 97.49% of the phase variance for A.S., 99.51% of the threshold amplitude and 96.65% of the phase variance for L.T.S., and 98.06% of the threshold amplitude and 92.49% of the phase variance for M.L. Relative to the mean of each set of data, the model accounts for 85.94% of the threshold amplitude and 85.51% of the phase variance for A.S., 95.10% of the threshold amplitude and 82.96% of the phase variance for L.T.S., and 86.76% of the threshold amplitude and 58.76% of the phase variance for M.L.

Figure 5 shows how the two adaptation-dependent parameters of the model depend upon the radiance of the 440-nm target for A.S. (gray triangles), L.T.S. (open squares), and M.L. (filled circles). The upper panel shows the time constants of each of the three filters, and the

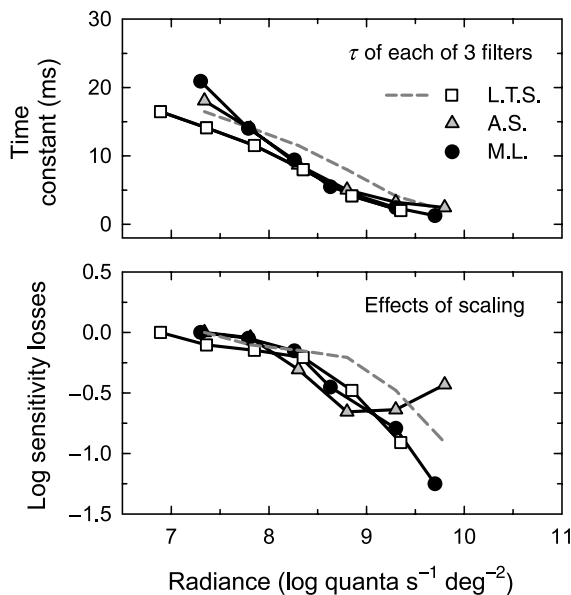


Figure 5. Adaptation-dependent model parameters for A.S. (gray triangles), L.T.S. (open squares), and M.L. (filled circles) for the two-parameter model. The parameters for L.T.S. have been shifted by 0.45 log unit along the abscissa. The unshifted values are shown by the gray dashed line. Upper panel: dependence of the time constant of each of the three integrating stages on the radiance of the 440-nm target in $\log \text{ quanta s}^{-1} \text{ deg}^{-2}$. Lower panel: cumulative logarithmic sensitivity losses assumed to be caused by multiplicative sensitivity scaling.

lower panel shows the *cumulative* changes in sensitivity scaling. The parameters for A.S. and M.L. exhibit a similar adaptation dependence, except for the change in scaling between the two highest levels. Between those levels, A.S. shows a marked loss in sensitivity, whereas M.L. shows a gain. We suspect that this difference arises because the saturation of the S-cone signal, as well as the associated loss in S-cone sensitivity, begins at the lower level of 9.80 for A.S. but not for M.L. The parameters for L.T.S. show a similar adaptation dependence to those for A.S. and M.L., except that L.T.S. is about 0.45 log unit less sensitive to the 440-nm target than either A.S. or M.L. This difference is probably due to prereceptor filtering (e.g., the lens pigment density) at 440 nm being greater in the oldest subject, L.T.S. The gray dashed lines in Figure 5 show the unshifted parameters for L.T.S., whereas the open squares show the parameters shifted along the log radiance scale by 0.45 log unit. After applying the shift, the parameters for all three subjects are fairly consistent. We conclude, therefore, that the mechanisms of S-cone adaptation in these three subjects are similar.

S-cone binocular phase lags

In our previous article wherein we investigated light adaptation (Stockman et al., 2006), we measured M-cone phase delays *binocularly* in protanopic observers. In this article, we measured S-cone phase delays relative to L/M-cone reference flicker *monocularly* in normal observers and in one protanope from the previous study. Monocular settings are much easier to make than binocular ones. Nevertheless, in one subject (L.T.S.), we measured S-cone phase delays monocularly and binocularly relative to S-cone reference flicker in the other eye. Binocular S-cone measures provide a useful control because they do not depend on interactions with L/M-cone signals in a common pathway, which we assume to be the luminance pathway (see above).

Binocular phase measurements depend on the well-established observation that binocular flicker is phase dependent and that different phases of flicker in both eyes can destructively interfere (e.g., Baker, 1952a, 1952b, 1952c, 1952d; Baker & Bott, 1951; Cavonius, 1979; Cavonius & Estévez, 1980; Ireland, 1951; Perrin, 1954; Sherrington, 1906; Thomas, 1954, 1955, 1956). As far as we are aware, binocular S-cone phase delays have not been measured before.

The binocular phase delays are shown as large colored symbols in Figure 6. They are restricted to lower frequencies than the monocular measurements, presumably because filtering prior to the cortical site of binocular cancellation limits the high-frequency signal that reaches the cancellation site. The binocular phase delays in the right eye were measured relative to the 8.80 $\log \text{ quanta s}^{-1} \text{ deg}^{-2}$ level in the left eye. As expected, those

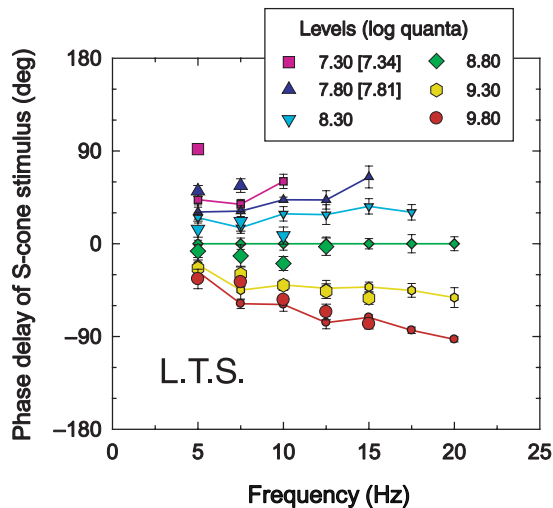


Figure 6. S-cone phase delays of signals generated in the right eye relative to those generated in the left eye for L.T.S. (large colored symbols) compared with S-cone phase delays measured monocularly relative to L/M-cone flicker from Figure 3 (small colored symbols and continuous lines). The 440-nm target in the left eye was fixed at 8.80 log quanta $s^{-1} \text{ deg}^{-2}$. The monocular phase data have been plotted relative to the phase delays for the 8.80 log quanta $s^{-1} \text{ deg}^{-2}$, 440-nm target to enable comparison. The color code in the key is used for all data.

measured at levels below 8.80 log quanta $s^{-1} \text{ deg}^{-2}$ are phase delayed, whereas those measured above it are phase advanced. The phase delays at 8.80 log quanta $s^{-1} \text{ deg}^{-2}$ are close to, but not precisely, 0° . These small deviations from 0° mean that the adaptive states of both eyes are slightly mismatched, despite receiving the same number of quanta at the cornea. A comparable mismatch was found in the binocular M-cone measurements (Stockman et al., 2006).

To allow comparisons between the binocular and monocular data, we have replotted the monocular data from Figure 2 but *relative to* the 8.80 log quanta $s^{-1} \text{ deg}^{-2}$ data (small colored symbols and solid lines). As can be seen, the monocular and binocular data are consistent, except at the lowest two levels. There, the binocular data are more phase delayed. This is an interesting discrepancy, which suggests that at the lowest levels, the reduction in phase delay may be somehow limited by the presence of the L/M-cone reference flicker—as might be the case if *postreceptoral* mechanisms of adaptation are important at those levels.

Discussion

The combination of amplitude and phase data presented here allow us to better constrain models of steady-state light adaptation than what has previously

been possible with psychophysical data. Like the M-cone data reported in our companion article, most of the variance in the S-cone data can be accounted for by a simple model with two adaptation-dependent parameters, which combines shortening time constants and sensitivity scaling.

The shortening integration time at lower levels and the decreasing sensitivity at higher levels are both in accord with other models of light adaptation (for reviews, see Graham & Hood, 1992; Hood, 1998; Hood & Finkelstein, 1986; MacLeod, 1978; Shapley & Enroth-Cugell, 1984). By contrast, the *increase* in overall sensitivity found at lower levels is counter to conventional psychophysical wisdom because adaptation is assumed to decrease sensitivity as the light level rises. The need for sensitivity increases becomes clear, however, when the perspective is changed to the molecular level (for reviews, see Arshavsky, Lamb, & Pugh, 2002; Burns & Baylor, 2001; Fain, Matthews, Cornwall, & Koutalos, 2001; Perlman & Normann, 1998; Pugh & Lamb, 2000; Pugh, Nikonov, & Lamb, 1999).

Molecular mechanisms of adaptation

For simplicity, we group the molecular mechanisms into three categories according to their likely *gross* overall effects on psychophysical measurements. Into the first category (A), we place mechanisms that are likely to speed up the visual response and shorten the visual integration time. Potential mechanisms are (i) the increase in the rate of cGMP hydrolysis mediated by the light-induced rise in the concentration of PDE6* (Hodgkin & Nunn, 1988; Nikonov, Engheta, & Pugh, 1998) and (ii) the decrease in the lifetime of R^* mediated by RK (Fain, Lamb, Matthews, & Murphy, 1989; Gray-Keller & Detwiler, 1996; Matthews, 1996, 1997; Murnick & Lamb, 1996; Torre, Matthews, & Lamb, 1986; Whitlock & Lamb, 1999). Into the second category (B), we place mechanisms that are likely to reduce overall sensitivity independently of temporal frequency and which are likely to have little effect on phase delay. Potential mechanisms are (i) pigment bleaching (e.g., Boynton & Whitten, 1970; Burkhardt, 1994; Hecht, 1937) and (ii) response compression caused by the availability of fewer CNG channels as the light level increases (Baylor & Hodgkin, 1974; Dowling & Ripps, 1970; Matthews, Murphy, Fain, & Lamb, 1988). Lastly, in the third category (C), we place mechanisms that are likely to increase overall sensitivity in a way that does not depend on temporal frequency and probably have little effect on phase delay. Potential mechanisms are (i) the increase in the rate of cGMP synthesis mediated by GC (Hodgkin & Nunn, 1988; Koutalos, Nakatani, Tamura, & Yau, 1995; Koutalos, Nakatani, & Yau, 1995; Koutalos & Yau, 1996; Polans, Baehr, & Palczewski, 1996; Pugh, Duda, Sitaramayya, & Sharma, 1997; Tamura, Nakatani, & Yau, 1991) and (ii)

the decrease in $K_{1/2}$ (the half-activation concentration) for cGMP, opening the CNG channels, which has the effect of making more channels available (Bauer, 1996; Chen et al., 1994; Grunwald, Yu, Yu, & Yau, 1998; Hsu & Molday, 1993, 1994; Rebrik & Korenbrot, 1998, 2004; Weitz et al., 1998).

When so categorized, the need for molecular mechanisms that increase sensitivity is clear. They are essential processes that act to restore depleted messenger molecules and increase the availability of limited ion channels. Without these processes, the visual response would quickly saturate as the molecules or channels run out. Their prevalence at the molecular level means that their signature should be apparent in these psychophysical S-cone data—as they are in M-cone data (Stockman et al., 2006).

S-cone model and the link to molecular mechanisms

Figure 7 shows the final form of the model based on the psychophysical data—with some embellishments. The first parameter of the model is the time constant of the three leaky integrators (A), which shorten together with adaptation (upper panel, Figure 5). The second parameter is multiplicative scaling (lower panel, Figure 5), which we have subdivided into scaling that reduces sensitivity (B) and scaling that increases sensitivity (C). Scaling that reduces sensitivity has been further subdivided into photopigment depletion (B_1), response compression (B_2), and other neural factors (B_3). Over the range of the S-cone measurements presented here, B_1 plays a minimal role. Although direct evidence about S-cone bleaching is unavailable, we estimate the 440-nm radiance at which half the S-cone photopigment is bleached to be approx-

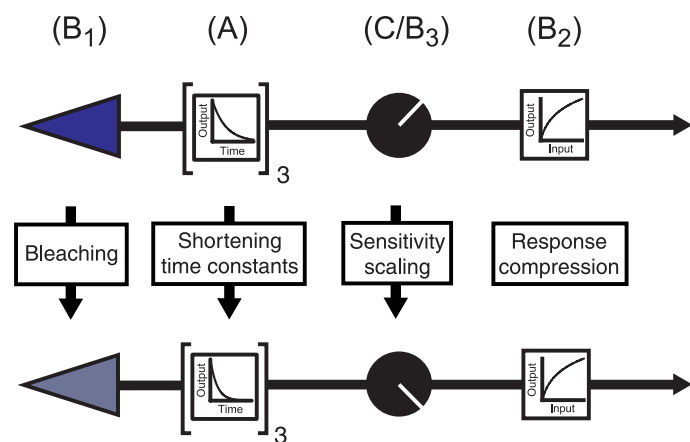


Figure 7. The final model made up of three leaky integrators (A), the time constants of which shorten together with adaptation, and sensitivity scaling. Sensitivity scaling is assumed to either increase (C) or decrease (B) sensitivity. Sensitivity scaling that decreases sensitivity is subdivided into photopigment bleaching (B_1), response compression (B_2), or other factors (B_3).

imately $10.70 \log \text{ quanta s}^{-1} \text{ deg}^{-2}$, which is well above the highest level used for modeling. This estimate is based on M- and L-cone half-bleaching estimates of $4.30 \log \text{ td}$ (Rushton & Henry, 1968) and assumes mean filtering by prereceptor filters at 440 nm (Stockman & Sharpe, 2000). For completeness, sensitivity scaling owing to response compression has been added as a separate element in the model (B_2). However, its effects, if any, cannot be distinguished in our data from those of other neural factors (B_3).

Each stage of the model can be loosely linked to the molecular processes just described. We can link the shortening time constants of the three filters to the two molecular mechanisms in Category A. As noted above, however, the number of filters is poorly constrained by the model fits. Thus, we cannot tell from our data whether only two molecular mechanisms might alone suffice to account for our data or whether other (as yet unknown) processes of receptor or postreceptor adaptation are also required.

From a psychophysical perspective, the most unexpected aspect of the model is that some scaling actually *increases* sensitivity. As can be seen in Figure 5, this reaches a cumulative gain in sensitivity of approximately 0.65, 0.91, and 1.25 log units for A.S., L.T.S., and M.L., respectively. We link these effects to the two molecular mechanisms noted under Category C. We note that the sensitivity gains due to these factors could be larger than model predictions because the gains could be offset by increases in scaling from Category B mechanisms, such as response compression caused by a reduction in open CNG channels. Postreceptor response compression probably plays a role in S-cone saturation at the highest adaptation levels (e.g., Pugh & Mollon, 1979).

We acknowledge the many previous attempts to model light adaptation, several of which incorporate some or all of the elements used in our model. These are discussed in our earlier article (Stockman et al., 2006) or in several excellent reviews on the topic (e.g., Graham & Hood, 1992; Hood, 1998; Hood & Finkelstein, 1986; MacLeod, 1978; Shapley & Enroth-Cugell, 1984). In the context of this article, there is great potential in a class of model that accounts for physiological and electroretinographic data by mathematically simulating the individual molecular steps in the rod or cone phototransduction cascade (e.g., Hamer, Nicholas, Tranchina, Lamb, & Jarvinen, 2005; Tranchina, Sneyd, & Cadenas, 1991; van Hateren, 2005). Although much more complex and detailed than the psychophysical model presented here, the molecular simulations should, at some level, be consistent with our psychophysical data.

Time constants and the number of filters

One limitation of the model is that it is difficult to determine unequivocally both the number of filters (n) and

the time constant of each filter (τ) because the two parameters interact in the model fits: An increase in one parameter can partially offset a decrease in the other (Stockman et al., 2006). We can illustrate the relationship between the two by comparing versions of the two-parameter model with different values of n . Figure 8 shows the best fitting values of τ for $n = 2$ (open inverted triangles), $n = 3$ (filled diamonds), and $n = 4$ (open triangles) filters for A.S. (upper panel), L.T.S. (middle panel), and M.L. (lower panel) plotted in double-logarithmic coordinates, which, with the exception of $n = 2$

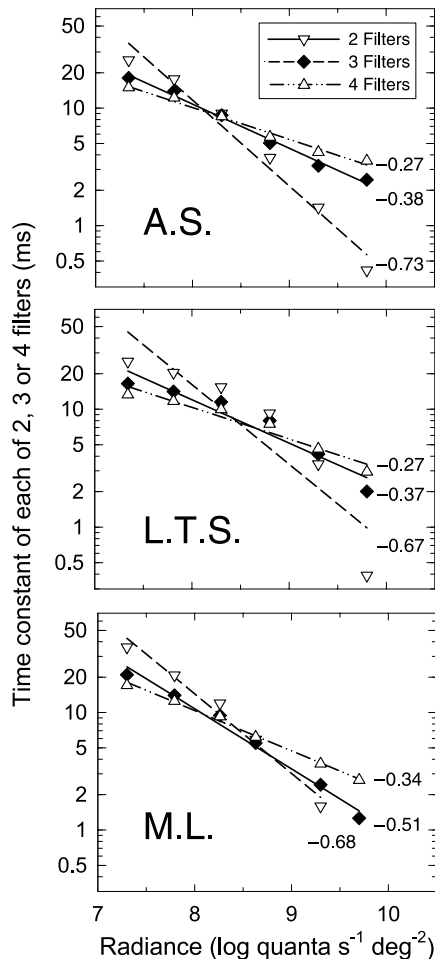


Figure 8. Time constants for each filter in milliseconds for versions of the two-adaptation-dependent-parameter model with two (open inverted triangles), three (filled diamonds), or four (open triangles) filters for A.S. (upper panel), L.T.S. (middle panel), and M.L. (lower panel). Each function can be approximated by a straight line in double-logarithmic coordinates, the best fitting versions of which are shown by the dashed (two filters), solid (three filters), and dotted–dashed (four filters) lines. The slopes of the best fitting lines are noted in the figure. The fits and model parameters shown in earlier figures correspond to the three-filter version of the model (see the [Time constants and the number of filters](#) section).

for L.T.S., account for the data plausibly well. As for the M-cone adaptation data and model (Stockman et al., 2006), the relationship between $\log(\tau)$ and \log luminance is approximately linear. Least squares linear regression provides the following estimates of the slopes: -0.73 , -0.38 , and -0.27 for $n = 2, 3$, and 4 , respectively, for A.S.; -0.67 , -0.37 , and -0.27 for L.T.S.; and -0.68 , -0.51 , and -0.34 for M.L.

We note that the fits to the data for $n = 2$ are problematical at the highest radiances. This arises because the time constants for $n = 2$ at approximately $9.80 \log \text{ quanta s}^{-1} \text{ deg}^{-2}$ are so short that the effect of varying them is similar to the effect of sensitivity scaling (over the visible range of frequencies). Thus, the two parameters can offset each other implausibly to account for small discrepancies in the data. The time constant for L.T.S. for $n = 2$ at $9.80 \log \text{ quanta s}^{-1} \text{ deg}^{-2}$ is shorter (0.39 ms) than might be expected from the other fits, whereas that for M.L. is so implausibly short (0.06 ms) that it was neither included in Figure 8 nor used to obtain the slope estimate. This problem aside, the mean slopes across n for S-cone adaptation are $-1.23/n$ for A.S., $-1.18/n$ for L.T.S., and $-1.40/n$ for M.L. These slopes provide an approximate *general* solution for how yoked time constants shorten with light adaptation for different values of n . They compare well with mean slopes for M-cone adaptation of $-1.37/n$ for M.L. and $-1.21/n$ for M.M. (Stockman et al., 2006).

Reconstructions of the amplitude thresholds and phase delays

The model fits shown in Figure 4 summarize the model predictions for the relative amplitude and phase differences. It is instructive to use the model to reconstruct the original data. Such reconstructions are shown in Figure 9 for A.S. (top panels), L.T.S. (middle panels), and M.L. (bottom panels). The reconstructions were achieved in three steps. First, the model was used to adjust each set of phase and amplitude data back to the *same* level of $9.80 \log \text{ quanta s}^{-1} \text{ deg}^{-2}$. Second, mean smoothed templates were derived separately for all the amplitude and phase data adjusted to the 9.80 level using a curve discovery program (TableCurve 2D, Jandel). Finally, the model predictions were used to adjust the smoothed templates for $9.80 \log \text{ quanta s}^{-1} \text{ deg}^{-2}$ back to each of the intensity levels. The templates adjusted for each level are shown as continuous lines in Figure 9. We attach no special significance to formulae for the template functions, which are not given.

The errors in the reconstruction are cumulative; hence, they should get worse as the level is decreased from $9.80 \log \text{ quanta s}^{-1} \text{ deg}^{-2}$. Although there are some discrepancies, the templates describe the data remarkably well over the entire range of levels.

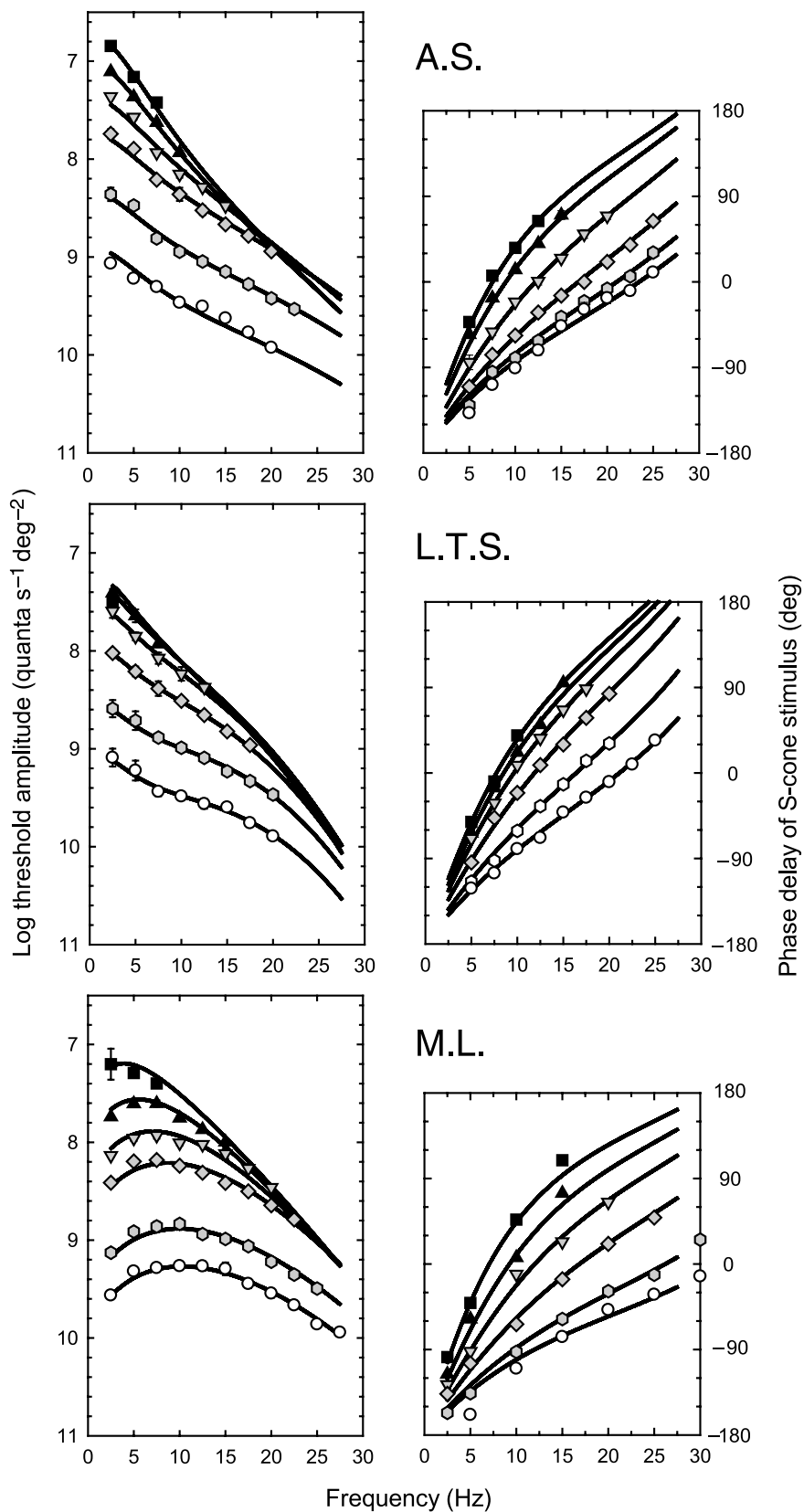


Figure 9. Logarithmic threshold amplitudes (symbols, left panels) and phase delays (symbols, right panels) for A.S. (top), L.T.S. (middle), and M.L. (bottom) and predictions of the two-parameter model reconstructed according to details in the text (solid lines). For key, see Figures 2, 3, and 4.

S-cone and M-cone model parameters compared

The protanopic observer M.L. was also the primary subject in our companion study of M-cone adaptation, for which the phase delays were measured binocularly. Figure 10 allows us to compare the model parameters for M.L. for M-cone (small filled circles) and S-cone (large open circles) adaptation. If the adaptation of the S- and M-cones and their respective pathways are mediated by the same underlying mechanisms, then the same model should account for both sets of data, differing only by a cone-specific scaling factor that reflects the difference in cone quantum catches resulting from the various targets and backgrounds. The M-cone parameters shown in Figure 10 have been shifted horizontally to align with the S-cone parameters. To interpret the shifts, we converted the S- and M-cone adaptation levels into equivalent quanta at λ_{\max} (541 nm for the M-cones and 441 nm for the S-cones) using the Stockman and Sharpe (2000) cone fundamentals. The abscissa is correct for S-cone quanta at λ_{\max} . The M-cone parameters have been horizontally shifted rightward by 0.10 log unit, which suggests that the M-cones are 0.10 log unit more

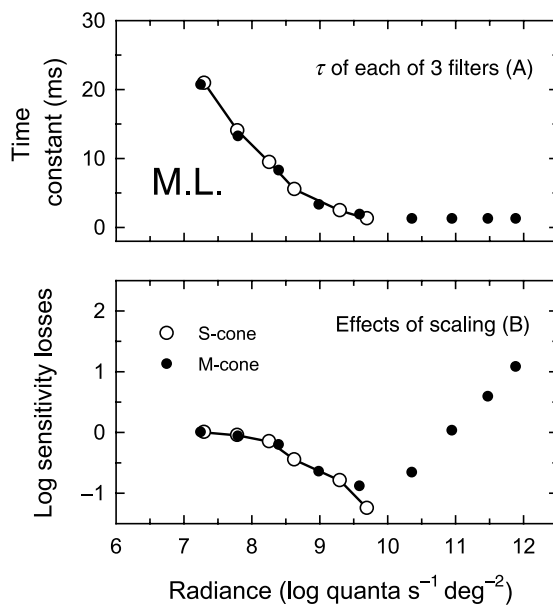


Figure 10. Model parameters for M.L. for S-cone-mediated adaptation (large open circles) compared with the parameters for his M-cone-mediated adaptation (small filled circles). The M-cone parameters have been shifted horizontally to align with the S-cone parameters as described in the text. Upper panel: dependence of the time constant of each of the three integrating stages on radiance. Lower panel: total cumulative logarithmic sensitivity losses found at low frequencies due to shortening time constants and all forms of sensitivity scaling. M-cone parameters are from Stockman et al. (2006).

sensitive at λ_{\max} than the S-cones. However, after taking into account the effects of filtering by the lens (c. 0.24 log unit more dense at 441 nm compared with 541 nm; see Table 1 of Stockman & Sharpe, 2000) and macular pigment (c. 0.29 log unit more dense at 441 nm for a 2° target; see Table 1 of Stockman & Sharpe, 2000, so that a lesser value of approximately 0.15 log unit might be reasonable for 4°, given that the density of the macular pigment decreases with eccentricity), the S-cones are actually approximately 0.29 log unit more sensitive to quanta at λ_{\max} than the M-cones. Such a difference might be consistent with the S-cones being, on average, larger than the M-cones over the 4° central area (e.g., Curcio et al., 1991) and, therefore, having a larger photon collecting aperture.

In summary, although the S-cone measurements are, of necessity, restricted to levels below S-cone saturation, in the region of overlap, the agreement, after allowing for M- and S-cone sensitivity differences at λ_{\max} , is remarkable. Thus, we conclude that the mechanisms of S- and M-cone adaptation in M.L. are similar, regardless of the details of our model. This correspondence strongly implies that the primary mechanisms of S- and M-cone adaptation must be in the S- and M-cone photoreceptors themselves, which are similar in biochemistry and physiology but not in their postreceptoral pathways (e.g., Dacey & Lee, 1994; Klug, Herr, Ngo, Sterling, & Schein, 2003; Kolb, Goede, Roberts, McDermott, & Gouras, 1997; Schein, Sterling, Ngo, Huang, & Herr, 2004).

Conclusions

The effects of light adaptation on both the S- and the M-cone responses can be accounted for by the same simple model, which is made up of a cascade of approximately three leaky integrators, the time constants of which shorten together with adaptation, and frequency-independent sensitivity scaling. Remarkably, the model requires just two adaptation-dependent parameters to account for the adaptation of the S-cones over 3 log units and of the M-cones over 5 log units.

Acknowledgments

This work was supported by a Wellcome Trust grant and, previously, by an NIH grant (EY10206) both awarded to A.S.

Commercial relationships: none.

Corresponding author: Andrew Stockman.

Email: a.stockman@ucl.ac.uk.

Address: Institute of Ophthalmology, University College London, 11-43 Bath Street, London EC1V 9EL, UK.

References

- Arshavsky, V. Y., Lamb, T. D., & Pugh, E. N., Jr. (2002). G proteins and phototransduction. *Annual Review of Physiology*, *64*, 153–187. [[PubMed](#)]
- Baker, C. H. (1952a). The dependence of binocular fusion on timing of peripheral stimuli and on central process: 1. Symmetrical flicker. *Canadian Journal of Psychology*, *6*, 1–10. [[PubMed](#)]
- Baker, C. H. (1952b). The dependence of binocular fusion on timing of peripheral stimuli and on central process: 1. Symmetrical flicker (continued). *Canadian Journal of Psychology*, *6*, 84–91. [[PubMed](#)]
- Baker, C. H. (1952c). The dependence of binocular fusion on timing of peripheral stimuli and on central process: 2. Asymmetrical flicker. *Canadian Journal of Psychology*, *6*, 123–130. [[PubMed](#)]
- Baker, C. H. (1952d). The dependence of binocular fusion on timing of peripheral stimuli and on central process: 3. Cortical flicker. *Canadian Journal of Psychology*, *6*, 151–163. [[PubMed](#)]
- Baker, C. H., & Bott, E. A. (1951). Studies on visual flicker and fusion: II. Effects of timing of visual stimuli on binocular fusion and flicker. *Canadian Journal of Psychology*, *5*, 9–17. [[PubMed](#)]
- Bauer, P. J. (1996). Cyclic GMP-gated channels of bovine rod photoreceptors: Affinity, density and stoichiometry of Ca(2+)-calmodulin binding sites. *The Journal of Physiology*, *494*, 675–685. [[PubMed](#)] [[Article](#)]
- Baylor, D. A., & Hodgkin, A. L. (1974). Changes in time scale and sensitivity in turtle photoreceptors. *Journal of Physiology*, *242*, 729–758. [[PubMed](#)] [[Article](#)]
- Boynton, R. M., & Whitten, D. N. (1970). Visual adaptation in monkey cones: Recordings of late receptor potentials. *Science*, *170*, 1423–1426. [[PubMed](#)]
- Brindley, G. S., Du Croz, J. J., & Rushton, W. A. H. (1966). The flicker fusion frequency of the blue-sensitive mechanism of colour vision. *The Journal of Physiology*, *183*, 497–500. [[PubMed](#)] [[Article](#)]
- Burkhardt, D. A. (1994). Light adaptation and photopigment bleaching in cone photoreceptors in situ in the retina of the turtle. *The Journal of Neuroscience*, *14*, 1091–1105. [[PubMed](#)]
- Burns, M. E., & Baylor, D. A. (2001). Activation, deactivation and adaptation in vertebrate photoreceptor cells. *Annual Review of Neuroscience*, *24*, 779–805. [[PubMed](#)]
- Cavonius, C. R. (1979). Binocular interactions in flicker. *Quarterly Journal of Experimental Psychology*, *31*, 273–280. [[PubMed](#)]
- Cavonius, C. R., & Estévez, O. (1980). Applications of signal-processing methods in visual psychophysics. In M. Kunt & F. de Coulon (Eds.), *Signal processing: Theories and applications* (pp. 343–349). Amsterdam: North-Holland Publishing Company.
- Chen, T. Y., Illing, M., Molday, L. L., Hsu, Y. T., Yau, K. W., & Molday, R. S. (1994). Subunit 2 (or beta) of retinal rod cGMP-gated cation channel is a component of the 240-kDa channel-associated protein and mediates Ca(2+)-calmodulin modulation. *Proceedings of the National Academy of Sciences of the United States of America*, *91*, 11757–11761. [[PubMed](#)] [[Article](#)]
- Curcio, C. A., Allen, K. A., Sloan, K. R., Lerea, C. L., Hurley, J. B., Klock, I. B., et al. (1991). Distribution and morphology of human cone photoreceptors stained with anti-blue opsin. *Journal of Comparative Neurology*, *312*, 610–624. [[PubMed](#)]
- Dacey, D. M., & Lee, B. B. (1994). The ‘blue-on’ opponent pathway in primate retina originates from a distinct bistratified ganglion cell type. *Nature*, *367*, 731–735. [[PubMed](#)]
- De Lange, H. (1958). Research into the dynamic nature of the human fovea-cortex systems with intermittent and modulated light: I. Attenuation characteristics with white and colored light. *Journal of the Optical Society of America*, *48*, 777–784.
- De Lange, H. (1961). Eye’s response at flicker fusion to square-wave modulation of a test field surrounded by a large steady field of equal mean luminance. *Journal of the Optical Society of America*, *51*, 415–421.
- Dowling, J. E., & Ripps, H. (1970). Visual adaptation in the retina of the skate. *Journal of General Physiology*, *56*, 491–520. [[PubMed](#)] [[Article](#)]
- Fain, G. L., Lamb, T. D., Matthews, H. R., & Murphy, R. L. (1989). Cytoplasmic calcium as the messenger for light adaptation in salamander rods. *The Journal of Physiology*, *416*, 215–243. [[PubMed](#)] [[Article](#)]
- Fain, G. L., Matthews, H. R., Cornwall, M. C., & Koutalos, Y. (2001). Adaptation in vertebrate photoreceptors. *Physiological Reviews*, *80*, 117–151. [[PubMed](#)] [[Article](#)]
- Graham, N., & Hood, D. C. (1992). Modeling the dynamics of adaptation: The merging of two traditions. *Vision Research*, *32*, 1373–1393. [[PubMed](#)]
- Gray-Keller, M. P., & Detwiler, P. B. (1996). Ca²⁺ dependence of dark- and light-adapted flash responses in rod photoreceptors. *Neuron*, *17*, 323–331. [[PubMed](#)] [[Article](#)]
- Green, D. G. (1968). The contrast sensitivity of the colour mechanisms of the human eye. *The Journal of Physiology*, *196*, 415–429. [[PubMed](#)] [[Article](#)]

- Green, D. G. (1969). Sinusoidal flicker characteristics of the colour-sensitive mechanisms of the eye. *Vision Research*, *9*, 591–601. [PubMed]
- Grunwald, M. E., Yu, W. P., Yu, H. H., & Yau, K. W. (1998). Identification of a domain on the beta-subunit of the rod cGMP-gated cation channel that mediates inhibition by calcium-calmodulin. *Journal of Biological Chemistry*, *273*, 9148–9157. [PubMed] [Article]
- Hamer, R. D., Nicholas, S. C., Tranchina, D., Lamb, T. D., & Jarvinen, J. L. P. (2005). Toward a unified model of vertebrate rod phototransduction. *Visual Neuroscience*, *22*, 417–436. [PubMed] [Article]
- Hecht, S. (1937). Rods, cones and the chemical basis of vision. *Physiological Reviews*, *17*, 239–290.
- Hodgkin, A. L., & Nunn, B. J. (1988). Control of light-sensitive current in salamander rods. *The Journal of Physiology*, *403*, 439–471. [PubMed] [Article]
- Hood, D. C. (1998). Lower-level visual processing and models of light adaptation. *Annual Review of Psychology*, *49*, 503–535. [PubMed]
- Hood, D. C., & Finkelstein, M. A. (1986). Sensitivity to light. In K. Boff, L. Kaufman, & J. Thomas (Eds.), *Handbook of perception and human performance* (vol. 1, pp. 5-1–5-66). New York: Wiley.
- Hsu, Y. T., & Molday, R. S. (1993). Modulation of the cGMP-gated channel of rod photoreceptor cells by calmodulin. *Nature*, *361*, 76–79. [PubMed]
- Hsu, Y. T., & Molday, R. S. (1994). Interaction of calmodulin with the cyclic GMP-gated channel of rod photoreceptor cells. Modulation of activity, affinity purification, and localization. *Journal of Biological Chemistry*, *269*, 29765–29770. [PubMed] [Article]
- Ireland, F. H. (1951). A comparison of critical flicker frequencies under conditions of monocular and binocular stimulation. *Journal of Experimental Psychology*, *40*, 282–286. [PubMed]
- Kelly, D. H. (1961). Visual responses to time-dependent stimuli: I. Amplitude sensitivity measurements. *Journal of the Optical Society of America*, *51*, 422–429. [PubMed]
- Kelly, D. H. (1974). Spatio-temporal frequency characteristics of color-vision mechanisms. *Journal of the Optical Society of America*, *64*, 983–990.
- Klug, K., Herr, S., Ngo, I. T., Sterling, P., & Schein, S. (2003). Macaque retina contains an S-cone OFF midwedge pathway. *The Journal of Neuroscience*, *23*, 9881–9887. [PubMed] [Article]
- Kolb, H., Goede, P., Roberts, S., McDermott, R., & Gouras, P. (1997). The uniqueness of the S-cone pedicle in the human retina and consequences for color processing. *Journal of Comparative Neurology*, *386*, 443–460. [PubMed]
- Koutalos, Y., Nakatani, K., Tamura, T., & Yau, K.-W. (1995). Characterization of guanylate cyclase activity in single retinal rod outer segments. *Journal of General Physiology*, *106*, 863–890. [PubMed] [Article]
- Koutalos, Y., Nakatani, K., & Yau, K.-W. (1995). The cGMP-phosphodiesterase and its contribution to sensitivity regulation in retinal rods. *Journal of General Physiology*, *106*, 891–921. [PubMed] [Article]
- Koutalos, Y., & Yau, K. W. (1996). Regulation of sensitivity in vertebrate rod photoreceptors by calcium. *Trends in Neurosciences*, *19*, 73–81. [PubMed]
- Lee, J., & Stromeyer, C. F., III. (1989). Contribution of human short-wave cones to luminance and motion detection. *The Journal of Physiology*, *413*, 563–593. [PubMed] [Article]
- Lit, A. (1949). The magnitude of the Pulfrich stereophenomenon as a function of binocular differences of intensity at various levels of illumination. *American Journal of Psychology*, *62*, 159–181.
- MacLeod, D. I. (1978). Visual sensitivity. *Annual Review of Psychology*, *29*, 613–645. [PubMed]
- Matin, L. (1968). Critical duration, the differential luminance threshold, critical flicker frequency, and visual adaptation: A theoretical treatment. *Journal of the Optical Society of America*, *58*, 404–415. [PubMed]
- Matthews, H. R. (1996). Static and dynamic actions of cytoplasmic Ca²⁺ in the adaptation of responses to saturating flashes in salamander rods. *The Journal of Physiology*, *490*, 1–15. [PubMed] [Article]
- Matthews, H. R. (1997). Actions of Ca²⁺ on an early stage in phototransduction revealed by the dynamic fall in Ca²⁺ concentration during the bright flash response. *Journal of General Physiology*, *109*, 141–146. [PubMed] [Article]
- Matthews, H. R., Murphy, R. L., Fain, G. L., & Lamb, T. D. (1988). Photoreceptor light adaptation is mediated by cytoplasmic calcium concentration. *Nature*, *334*, 67–69. [PubMed]
- Mollon, J. D., & Polden, P. G. (1977). Saturation of a retinal cone mechanism. *Nature*, *259*, 243–246. [PubMed]
- Murnick, J. G., & Lamb, T. D. (1996). Kinetics of desensitization induced by saturating flashes in toad and salamander rods. *The Journal of Physiology*, *495*, 1–13. [PubMed] [Article]
- Nikonov, S., Engheta, N., & Pugh, E. N., Jr. (1998). Kinetics of recovery of the dark-adapted salamander

- rod photoresponse. *Journal of General Physiology*, *111*, 7–37. [PubMed] [Article]
- Perlman, I., & Normann, R. A. (1998). Light adaptation and sensitivity controlling mechanisms in vertebrate photoreceptors. *Progress in Retinal and Eye Research*, *17*, 523–563. [PubMed]
- Perrin, F. H. (1954). A study in binocular flicker. *Journal of the Optical Society of America*, *44*, 60–69. [PubMed]
- Polans, A., Baehr, W., & Palczewski, K. (1996). Turned on by Ca²⁺! The physiology and pathology of Ca(2+)-binding proteins in the retina. *Trends in Neurosciences*, *19*, 547–554. [PubMed]
- Pugh, E. N., Jr., Duda, T., Sitaramayya, A., & Sharma, R. K. (1997). Photoreceptor guanylate cyclases: A review. *Bioscience Reports*, *17*, 429–473. [PubMed]
- Pugh, E. N., Jr., & Lamb, T. D. (2000). Phototransduction in vertebrate rods and cones: Molecular mechanisms of amplification, recovery and light adaptation. In D. G. Stavenga, W. J. de Grip, & E. N. Pugh (Eds.), *Handbook of biological physics: Vol. 3. Molecular mechanisms of visual transduction* (pp. 183–255). Amsterdam: Elsevier.
- Pugh, E. N., Jr., & Mollon, J. D. (1979). A theory of the p1 and p3 color mechanisms of Stiles. *Vision Research*, *20*, 293–312. [PubMed]
- Pugh, E. N., Jr., Nikonov, S., & Lamb, T. D. (1999). Molecular mechanisms of vertebrate photoreceptor light adaptation. *Current Opinion in Neurobiology*, *9*, 410–418. [PubMed]
- Pulfrich, C. (1922). Die Stereskopie im Dienste der isochromen und heterochromen Photometrie. *Naturwissenschaften*, *10*, 553–564, 569–574, 596–601, 714–722, 735–743, 751–761.
- Rebrik, T. I., & Korenbrot, J. I. (1998). In intact cone photoreceptors, a Ca²⁺-dependent, diffusible factor modulates the cGMP-gated ion channels differently than in rods. *Journal of General Physiology*, *112*, 537–548. [PubMed] [Article]
- Rebrik, T. I., & Korenbrot, J. I. (2004). In intact mammalian photoreceptors, Ca²⁺-dependent modulation of cGMP-gated ion channels is detectable in cones but not in rods. *Journal of General Physiology*, *123*, 63–75. [PubMed] [Article]
- Rock, M. L., & Fox, B. H. (1949). Two aspects of the Pulfrich phenomenon. *American Journal of Psychology*, *62*, 279–284.
- Rushton, W. A. H., & Henry, G. H. (1968). Bleaching and regeneration of cone pigments in man. *Vision Research*, *8*, 617–631. [PubMed]
- Schein, S., Sterling, P., Ngo, I. T., Huang, T. M., & Herr, S. (2004). Evidence that each S cone in macaque fovea drives one narrow-field and several wide-field blue–yellow ganglion cells. *The Journal of Neuroscience*, *24*, 8366–8378. [PubMed] [Article]
- Shapley, R., & Enroth-Cugell, C. (1984). Visual adaptation and retinal gain controls. In N. Osborne & G. Chader (Eds.), *Progress in retinal research* (vol. 3, pp. 263–346). New York: Pergamon Press.
- Sharpe, L. T., Stockman, A., Jagla, W., & Jägle, H. (2005). A luminous efficiency function, V*(λ), for daylight adaptation. *Journal of Vision*, *5*(11):3, 948–968, <http://journalofvision.org/5/11/3/>, doi:10.1167/5.11.3. [PubMed] [Article]
- Sharpe, L. T., Stockman, A., Jägle, H., Knau, H., Klausen, G., Reitner, A., et al. (1998). Red, green, and red–green hybrid pigments in the human retina: Correlations between deduced protein sequences and psychophysically measured spectral sensitivities. *The Journal of Neuroscience*, *18*, 10053–10069. [PubMed] [Article]
- Sherrington, C. S. (1906). *The integrative action of the nervous system*. New Haven: Yale University Press.
- Sperling, G., & Sondhi, M. M. (1968). Model for visual luminance discrimination and flicker detection. *Journal of the Optical Society of America*, *58*, 1133–1145. [PubMed]
- Stockman, A., Langendörfer, M., Smithson, H. E., & Sharpe, L. T. (2006). Human cone light adaptation: from behavioral measurements to molecular mechanisms. *Journal of Vision*, *6*(11):5, 1194–1213, <http://journalofvision.org/6/11/5/>, doi:10.1167/6.11.5. [PubMed] [Article]
- Stockman, A., MacLeod, D. I. A., & DePriest, D. D. (1987). An inverted S-cone input to the luminance channel: Evidence for two processes in S-cone flicker detection. *Investigative Ophthalmology and Visual Science*, *28*(Suppl.), 92.
- Stockman, A., MacLeod, D. I. A., & DePriest, D. D. (1991). The temporal properties of the human short-wave photoreceptors and their associated pathways. *Vision Research*, *31*, 189–208. [PubMed]
- Stockman, A., MacLeod, D. I. A., & Lebrun, S. J. (1993). Faster than the eye can see: Blue cones respond to rapid flicker. *Journal of the Optical Society of America A, Optics and Image Science*, *10*, 1396–1402. [PubMed]
- Stockman, A., & Plummer, D. J. (1998). Color from invisible flicker: A failure of the Talbot–Plateau law caused by an early ‘hard’ saturating nonlinearity used to partition the human short-wave cone pathway. *Vision Research*, *38*, 3703–3728. [PubMed]
- Stockman, A., & Sharpe, L. T. (2000). Spectral sensitivities of the middle- and long-wavelength sensitive cones derived from measurements in observers of

- known genotype. *Vision Research*, *40*, 1711–1737. [[PubMed](#)]
- Stromeyer, C. F., III, Kronauer, R. E., & Madsen, J. C. (1979). Response saturation of short-wavelength cone pathways controlled by color-opponent mechanisms. *Vision Research*, *19*, 1025–1040. [[PubMed](#)]
- Tamura, T., Nakatani, K., & Yau, K. W. (1991). Calcium feedback and sensitivity in primate rods. *Journal of General Physiology*, *98*, 95–130. [[PubMed](#)] [[Article](#)]
- Thomas, G. J. (1954). The effect on critical flicker frequency of interocular differences in intensity and in phase relations of flashes of light. *American Journal of Psychology*, *67*, 632–646. [[PubMed](#)]
- Thomas, G. J. (1955). A comparison of unocular and binocular critical flicker frequencies: Simultaneous and alternate flashes. *American Journal of Psychology*, *68*, 37–53. [[PubMed](#)]
- Thomas, G. J. (1956). Effect of contours on binocular CFF obtained with synchronous and alternate flashes. *American Journal of Psychology*, *69*, 369–377. [[PubMed](#)]
- Torre, V., Matthews, H. R., & Lamb, T. D. (1986). Role of calcium in regulating the cyclic GMP cascade of phototransduction in retinal rods. *Proceedings of the National Academy of Sciences of the United States of America*, *83*, 7109–7113. [[PubMed](#)] [[Article](#)]
- Tranchina, D., Gordon, J., & Shapley, R. M. (1984). Retinal light adaptation-evidence for a feedback mechanism. *Nature*, *310*, 314–316. [[PubMed](#)]
- Tranchina, D., Sneyd, J., & Cadenas, I. D. (1991). Light adaptation in turtle cones: Testing and analysis of a model for phototransduction. *Biophysical Journal*, *60*, 217–237. [[PubMed](#)] [[Article](#)]
- van Hateren, H. (2005). A cellular and molecular model of response kinetics and adaptation in primate cones and horizontal cells. *Journal of Vision*, *5*(4):5, 331–347, <http://journalofvision.org/5/4/5/>, doi:10.1167/5.4.5. [[PubMed](#)] [[Article](#)]
- Watson, A. B. (1986). Temporal sensitivity. In K. Boff, L. Kaufman, & J. Thomas (Eds.), *Handbook of perception and human performance* (vol. 1, pp. 6-1–6-43). New York: Wiley.
- Weitz, D., Zoche, M., Muller, F., Beyermann, M., Korschen, H. G., Kaupp, U. B., et al. (1998). Calmodulin controls the rod photoreceptor CNG channel through an unconventional binding site in the N-terminus of the beta-subunit. *European Molecular Biology Organization Journal*, *17*, 2273–2284. [[PubMed](#)] [[Article](#)]
- Whitlock, G. G., & Lamb, T. D. (1999). Variability in the time course of single photon responses from toad rods: Termination of rhodopsin's activity. *Neuron*, *23*, 337–351. [[PubMed](#)] [[Article](#)]
- Wilson, J. A., & Anstis, S. M. (1969). Visual delay as a function of luminance. *American Journal of Psychology*, *82*, 350–358. [[PubMed](#)]
- Wisowaty, J. J., & Boynton, R. M. (1980). Temporal modulation sensitivity of the blue mechanism: Measurements made without chromatic adaptation. *Vision Research*, *20*, 895–909. [[PubMed](#)]